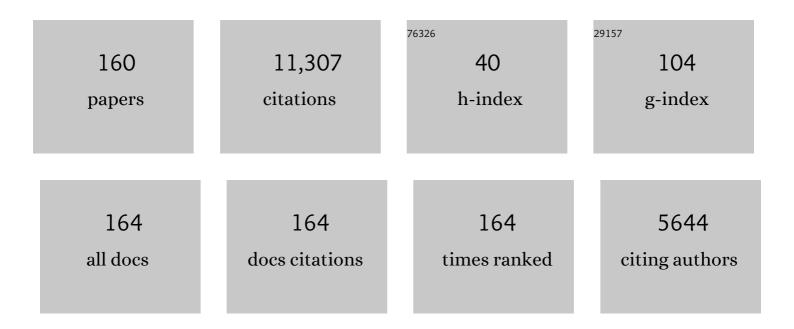
## Jan Henrik Ardenkjær-Larsen

List of Publications by Year in descending order

Source: https://exaly.com/author-pdf/558873/publications.pdf Version: 2024-02-01



#	Article	IF	CITATIONS
1	Metabolism of hyperpolarised [1– <sup>13</sup> C]pyruvate in awake and anaesthetised rat brains. NMR in Biomedicine, 2022, 35, e4635.	2.8	7
2	[68Ga]Ga-NODAGA-E[(cRGDyK)]2 PET and hyperpolarized [1-13C] pyruvate MRSI (hyperPET) in canine cancer patients: simultaneous imaging of angiogenesis and the Warburg effect. European Journal of Nuclear Medicine and Molecular Imaging, 2021, 48, 395-405.	6.4	8
3	Threeâ€element matching networks for receiveâ€only MRI coil decoupling. Magnetic Resonance in Medicine, 2021, 85, 544-550.	3.0	3
4	Hyperpolarization via dissolution dynamic nuclear polarization: new technological and methodological advances. Magnetic Resonance Materials in Physics, Biology, and Medicine, 2021, 34, 5-23.	2.0	32
5	Hyperpolarization by Dissolution Dynamic Nuclear Polarization. , 2021, , 1-26.		0
6	Radio Frequency Coils for Hyperpolarized 13C Magnetic Resonance Experiments with a 3T MR Clinical Scanner: Experience from a Cardiovascular Lab. Electronics (Switzerland), 2021, 10, 366.	3.1	2
7	Metabolic MRI with hyperpolarized [1- <sup>13</sup> C]pyruvate separates benign oligemia from infarcting penumbra in porcine stroke. Journal of Cerebral Blood Flow and Metabolism, 2021, 41, 2916-2927.	4.3	10
8	Direct measurement of the triple spin flip rate in dynamic nuclear polarization. Journal of Magnetic Resonance, 2021, 327, 106982.	2.1	4
9	Metabolic contrast agents produced from transported solid 13C-glucose hyperpolarized via dynamic nuclear polarization. Communications Chemistry, 2021, 4, .	4.5	17
10	Real-Time insight into in vivo redox status utilizing hyperpolarized [1-13C] N-acetyl cysteine. Scientific Reports, 2021, 11, 12155.	3.3	6
11	Classification and biomarker identification of prostate tissue from TRAMP mice with hyperpolarized 13C-SIRA. Talanta, 2021, 235, 122812.	5.5	11
12	Pilot Study Experiences With Hyperpolarized [1â€ <sup>13</sup> C]pyruvate MRI in Pancreatic Cancer Patients. Journal of Magnetic Resonance Imaging, 2020, 51, 961-963.	3.4	45
13	Detection of lentiviral suicide gene therapy in C6 rat glioma using hyperpolarised [1―13 C]pyruvate. NMR in Biomedicine, 2020, 33, e4250.	2.8	3
14	Autonomous cryogenic RF receive coil for <sup>13</sup> C imaging of rodents at 3 T. Magnetic Resonance in Medicine, 2020, 84, 497-508.	3.0	9
15	Pancreatic β-cells respond to fuel pressure with an early metabolic switch. Scientific Reports, 2020, 10, 15413.	3.3	5
16	Multi-site benchmarking of clinical 13C RF coils at 3T. Journal of Magnetic Resonance, 2020, 318, 106798.	2.1	10
17	<sup>13</sup> C Dynamic Nuclear Polarization using SA-BDPA at 6.7 T and 1.1 K: Coexistence of Pure Thermal Mixing and Well-Resolved Solid Effect. Journal of Physical Chemistry Letters, 2020, 11, 6873-6879.	4.6	7
18	Unexpected Anomeric Acceptor Preference Observed Using dDNP NMR for Transglycosylation Studies of β-Galactosidases. Biochemistry, 2020, 59, 2903-2908.	2.5	5

#	Article	IF	CITATIONS
19	Matching and decoupling networks for receive-only MRI arrays. , 2020, , .		3
20	UV-Irradiated 2-Keto-(1- <sup>13</sup> C)Isocaproic Acid for High-Performance <sup>13</sup> C Hyperpolarized MR. Journal of Physical Chemistry C, 2020, 124, 23859-23866.	3.1	4
21	Hyperpolarized water through dissolution dynamic nuclear polarization with UV-generated radicals. Communications Chemistry, 2020, 3, .	4.5	30
22	Threeâ€dimensional accelerated acquisition for hyperpolarized 13 C MR with blipped stackâ€ofâ€spirals and conjugateâ€gradient SENSE. Magnetic Resonance in Medicine, 2020, 84, 519-534.	3.0	5
23	Creating a clinical platform for carbonâ€13 studies using the sodiumâ€23 and proton resonances. Magnetic Resonance in Medicine, 2020, 84, 1817-1827.	3.0	24
24	Stable isotope resolved metabolomics classification of prostate cancer cells using hyperpolarized NMR data. Journal of Magnetic Resonance, 2020, 316, 106750.	2.1	16
25	Three-spin solid effect and the spin diffusion barrier in amorphous solids. Science Advances, 2019, 5, eaax2743.	10.3	47
26	Coil profile estimation strategies for parallel imaging with hyperpolarized 13 C MRI. Magnetic Resonance in Medicine, 2019, 82, 2104-2117.	3.0	9
27	Hyperpolarized MR – What's up Doc?. Journal of Magnetic Resonance, 2019, 306, 124-127.	2.1	17
28	Gadolinium Effect at High-Magnetic-Field DNP: 70% <sup>13</sup> C Polarization of [U- <sup>13</sup> C] Glucose Using Trityl. Journal of Physical Chemistry Letters, 2019, 10, 3420-3425.	4.6	30
29	Optimized microwave delivery in dDNP. Journal of Magnetic Resonance, 2019, 305, 58-65.	2.1	7
30	Design of a local quasi-distributed tuning and matching circuit for dissolution DNP cross polarization. Solid State Nuclear Magnetic Resonance, 2019, 102, 12-20.	2.3	13
31	Compact, low-cost NMR spectrometer and probe for dissolution DNP. Journal of Magnetic Resonance, 2019, 304, 7-15.	2.1	4
32	Dynamic Imaging of Glucose and Lactate Metabolism by 13C-MRS without Hyperpolarization. Scientific Reports, 2019, 9, 3410.	3.3	56
33	Real-Time Detection of Intermediates in Rhodium-Catalyzed Hydrogenation of Alkynes and Alkenes by Dissolution DNP. Journal of Physical Chemistry C, 2019, 123, 9949-9956.	3.1	15
34	PIN diode driver for NMR and MRI. Journal of Magnetic Resonance, 2019, 300, 114-119.	2.1	2
35	Rapid zero-trans kinetics of Cs+ exchange in human erythrocytes quantified by dissolution hyperpolarized 133Cs+ NMR spectroscopy. Scientific Reports, 2019, 9, 19726.	3.3	4
36	Magnetic resonance imaging with optical preamplification and detection. Scientific Reports, 2019, 9, 18173.	3.3	13

#	Article	IF	CITATIONS
37	Improved Decoupling for Low Frequency MRI Arrays Using Non-Conventional Preamplifier Impedance. IEEE Transactions on Biomedical Engineering, 2019, 66, 1940-1948.	4.2	10
38	Hyperpolarized 13C MRI: Path to Clinical Translation in Oncology. Neoplasia, 2019, 21, 1-16.	5.3	316
39	Cryogenâ€free dissolution dynamic nuclear polarization polarizer operating at 3.35 T, 6.70 T, and 10.1 T. Magnetic Resonance in Medicine, 2019, 81, 2184-2194.	3.0	85
40	Efficient Hyperpolarization of Uâ€ <sup>13</sup> Câ€Glucose Using Narrowâ€Line UVâ€Generated Labile Free Radicals. Angewandte Chemie, 2019, 131, 1348-1353.	2.0	4
41	Efficient Hyperpolarization of Uâ€≺sup>13Câ€Glucose Using Narrowâ€Line UVâ€Generated Labile Free Radicals. Angewandte Chemie - International Edition, 2019, 58, 1334-1339.	13.8	35
42	Targeted Metabolomics with Quantitative Dissolution Dynamic Nuclear Polarization. Methods in Molecular Biology, 2019, 2037, 385-393.	0.9	6
43	Sensitive optomechanical transduction of electric and magnetic signals to the optical domain. Optics Express, 2019, 27, 18561.	3.4	13
44	High Intrarenal Lactate Production Inhibits the Renal Pseudohypoxic Response to Acutely Induced Hypoxia in Diabetes. Tomography, 2019, 5, 239-247.	1.8	4
45	Imaging of glucose metabolism by 13C-MRI distinguishes pancreatic cancer subtypes in mice. ELife, 2019, 8, .	6.0	19
46	Cryogenic Preamplifiers for Magnetic Resonance Imaging. IEEE Transactions on Biomedical Circuits and Systems, 2018, 12, 202-210.	4.0	9
47	Discovery of Intermediates of lacZ β-Galactosidase Catalyzed Hydrolysis Using dDNP NMR. Journal of the American Chemical Society, 2018, 140, 3030-3034.	13.7	12
48	Molecular imaging of tumor photoimmunotherapy: Evidence of photosensitized tumor necrosis and hemodynamic changes. Free Radical Biology and Medicine, 2018, 116, 1-10.	2.9	16
49	Dynamic coronary MR angiography in a pig model with hyperpolarized water. Magnetic Resonance in Medicine, 2018, 80, 1165-1169.	3.0	12
50	Liquid-State <sup>13</sup> C Polarization of 30% through Photoinduced Nonpersistent Radicals. Journal of Physical Chemistry C, 2018, 122, 7432-7443.	3.1	34
51	Stable Isotope-Resolved Analysis with Quantitative Dissolution Dynamic Nuclear Polarization. Analytical Chemistry, 2018, 90, 674-678.	6.5	32
52	Association and Dissociation of Optimal Noise and Input Impedance for Low-Noise Amplifiers. IEEE Transactions on Microwave Theory and Techniques, 2018, 66, 5290-5299.	4.6	3
53	Development of a Symmetric Echo-Planar Spectroscopy Imaging Framework for Hyperpolarized 13C Imaging in a Clinical PET/MR Scanner. Tomography, 2018, 4, 110-122.	1.8	5
54	Combined hyperpolarized 13C-pyruvate MRS and 18F-FDG PET (hyperPET) estimates of glycolysis in canine cancer patients. European Journal of Radiology, 2018, 103, 6-12.	2.6	21

#	Article	IF	CITATIONS
55	Fumarase activity: an in vivo and in vitro biomarker for acute kidney injury. Scientific Reports, 2017, 7, 40812.	3.3	38
56	Antioxidant treatment attenuates lactate production in diabetic nephropathy. American Journal of Physiology - Renal Physiology, 2017, 312, F192-F199.	2.7	28
57	Hyperpolarized <sup>133</sup> Cs is a sensitive probe for real-time monitoring of biophysical environments. Chemical Communications, 2017, 53, 6625-6628.	4.1	7
58	Simultaneous imaging of hyperpolarized [1,4â€ <sup>13</sup> C <sub>2</sub> ]fumarate, [1â€ <sup>13</sup> C]pyruvate and <sup>18</sup> F–FDG in a rat model of necrosis in a clinical PET/MR scanner. NMR in Biomedicine, 2017, 30, e3803.	2.8	13
59	Renal <scp>MR</scp> angiography and perfusion in the pig using hyperpolarized water. Magnetic Resonance in Medicine, 2017, 78, 1131-1135.	3.0	18
60	Large dose hyperpolarized water with dissolution-DNP at high magnetic field. Journal of Magnetic Resonance, 2017, 274, 65-72.	2.1	29
61	Towards new vistas in preamplifier design for MRI. , 2017, , .		0
62	Low-Noise Active Decoupling Circuit and its Application to 13C Cryogenic RF Coils at 3 T. Tomography, 2017, 3, 60-66.	1.8	14
63	Imaging Regional Metabolic Changes in the Ischemic Rat Heart In Vivo Using Hyperpolarized [1-13C]Pyruvate. Tomography, 2017, 3, 123-130.	1.8	3
64	Waveguide transition with vacuum window for multiband dynamic nuclear polarization systems. Review of Scientific Instruments, 2016, 87, 054705.	1.3	5
65	Tunable 13C/1H dual channel matching circuit for dynamic nuclear polarization system with cross-polarization. , 2016, , .		2
66	Difference between Extra―and Intracellular <i>T</i> <sub>1</sub> Values of Carboxylic Acids Affects the Quantitative Analysis of Cellular Kinetics by Hyperpolarized NMR. Angewandte Chemie - International Edition, 2016, 55, 13567-13570.	13.8	12
67	Dissolution Dynamic Nuclear Polarization capability study with fluid path. Journal of Magnetic Resonance, 2016, 272, 141-146.	2.1	13
68	Difference between Extra―and Intracellular <i>T</i> <sub>1</sub> Values of Carboxylic Acids Affects the Quantitative Analysis of Cellular Kinetics by Hyperpolarized NMR. Angewandte Chemie, 2016, 128, 13765-13768.	2.0	4
69	Microwave-gated dynamic nuclear polarization. Physical Chemistry Chemical Physics, 2016, 18, 30530-30535.	2.8	42
70	Hyperpolarized 13 C urea relaxation mechanism reveals renal changes in diabetic nephropathy. Magnetic Resonance in Medicine, 2016, 75, 515-518.	3.0	34
71	On the present and future of dissolution-DNP. Journal of Magnetic Resonance, 2016, 264, 3-12.	2.1	197
72	Imaging Renal Urea Handling in Rats at Millimeter Resolution Using Hyperpolarized Magnetic Resonance Relaxometry. Tomography, 2016, 2, 125-137.	1.8	31

#	Article	IF	CITATIONS
73	A fast and simple method for calibrating the flip angle in hyperpolarized <sup>13</sup> <scp>C MRS</scp> experiments. Concepts in Magnetic Resonance Part B, 2015, 45, 78-84.	0.7	3
74	Realâ€ŧime cardiac metabolism assessed with hyperpolarized [1â€< sup>13C]acetate in a largeâ€animal model. Contrast Media and Molecular Imaging, 2015, 10, 194-202.	0.8	44
75	Facing and Overcoming Sensitivity Challenges in Biomolecular NMR Spectroscopy. Angewandte Chemie - International Edition, 2015, 54, 9162-9185.	13.8	258
76	Hyperpolarized 13C MR Angiography. Current Pharmaceutical Design, 2015, 22, 90-95.	1.9	5
77	Dissolution Dynamic Nuclear Polarization of Non-Self-Glassing Agents: Spectroscopy and Relaxation of Hyperpolarized [1- <sup>13</sup> C]Acetate. Journal of Physical Chemistry A, 2015, 119, 1885-1893.	2.5	17
78	Monitoring mammary tumor progression and effect of tamoxifen treatment in MMTVâ€PymT using MRI and magnetic resonance spectroscopy with hyperpolarized [1â€ <sup>13</sup> C]pyruvate. Magnetic Resonance in Medicine, 2015, 73, 51-58.	3.0	23
79	Simultaneous Hyperpolarized <sup>13</sup> C-Pyruvate MRI and <sup>18</sup> F-FDG PET (HyperPET) in 10 Dogs with Cancer. Journal of Nuclear Medicine, 2015, 56, 1786-1792.	5.0	54
80	Quantified p <scp>H</scp> imaging with hyperpolarized <sup>13</sup> <scp>C</scp> â€bicarbonate. Magnetic Resonance in Medicine, 2015, 73, 2274-2282.	3.0	36
81	Simulation and comparison of coils for Hyperpolarized 13 C MRS cardiac metabolism studies in pigs. Measurement: Journal of the International Measurement Confederation, 2015, 60, 78-84.	5.0	4
82	The use of dynamic nuclear polarization (13)C-pyruvate MRS in cancer. American Journal of Nuclear Medicine and Molecular Imaging, 2015, 5, 548-60.	1.0	32
83	High altitude may alter oxygen availability and renal metabolism in diabetics as measured by hyperpolarized [1-13C]pyruvate magnetic resonance imaging. Kidney International, 2014, 86, 67-74.	5.2	64
84	<i>In vivo</i> measurement of apparent diffusion coefficients of hyperpolarized <sup>13</sup> C-labeled metabolites. NMR in Biomedicine, 2014, 27, 561-569.	2.8	30
85	Simultaneous multiagent hyperpolarized <sup>13</sup> C perfusion imaging. Magnetic Resonance in Medicine, 2014, 72, 1599-1609.	3.0	50
86	Apparent rate constant mapping using hyperpolarized [1– <sup>13</sup> C]pyruvate. NMR in Biomedicine, 2014, 27, 1256-1265.	2.8	46
87	In vivo single-shot 13C spectroscopic imaging of hyperpolarized metabolites by spatiotemporal encoding. Journal of Magnetic Resonance, 2014, 240, 8-15.	2.1	38
88	Enhanced performance large volume dissolution-DNP. Journal of Magnetic Resonance, 2014, 240, 90-94.	2.1	9
89	A new RF tagging pulse based on the Frank poly-phase perfect sequence. Journal of Magnetic Resonance, 2014, 247, 50-53.	2.1	1
90	Storage of magnetization as singlet order by optimal control designed pulses. Magnetic Resonance in Medicine, 2014, 71, 921-926.	3.0	9

#	Article	IF	CITATIONS
91	Hyperpolarized H <sub>2</sub> O MR angiography. Magnetic Resonance in Medicine, 2014, 71, 50-56.	3.0	26
92	Insufficient insulin administration to diabetic rats increases substrate utilization and maintains lactate production in the kidney. Physiological Reports, 2014, 2, e12233.	1.7	39
93	Saturationâ€recovery metabolicâ€exchange rate imaging with hyperpolarized [1â€ <sup>13</sup> C] pyruvate using spectralâ€spatial excitation. Magnetic Resonance in Medicine, 2013, 69, 1209-1216.	3.0	76
94	EPR oxygen imaging and hyperpolarized <sup>13</sup> C MRI of pyruvate metabolism as noninvasive biomarkers of tumor treatment response to a glycolysis inhibitor 3â€bromopyruvate. Magnetic Resonance in Medicine, 2013, 69, 1443-1450.	3.0	44
95	Transmit-Only/Receive-Only Radiofrequency System for Hyperpolarized 13C MRS Cardiac Metabolism Studies in Pigs. Applied Magnetic Resonance, 2013, 44, 1125-1138.	1.2	5
96	3D cardiac Chemical Shift Imaging of [1-13C] hyperpolarized acetate and pyruvate in pigs. Journal of Cardiovascular Magnetic Resonance, 2013, 15, P10.	3.3	1
97	Assessment of early diabetic renal changes with hyperpolarized [1â€ <sup>13</sup> C]pyruvate. Diabetes/Metabolism Research and Reviews, 2013, 29, 125-129.	4.0	83
98	Magnetic resonance imaging of tumor oxygenation and metabolic profile. Acta Oncológica, 2013, 52, 1248-1256.	1.8	17
99	Field dependence of <i>T</i> <sub>1</sub> for hyperpolarized [1â€ <sup>13</sup> C]pyruvate. Contrast Media and Molecular Imaging, 2013, 8, 57-62.	0.8	45
100	Dynamic nuclear polarization and optimal control spatial-selective 13C MRI and MRS. Journal of Magnetic Resonance, 2013, 227, 57-61.	2.1	21
101	Efficiency evaluation of a 13C Magnetic Resonance birdcage coil: Theory and comparison of four methods. Measurement: Journal of the International Measurement Confederation, 2013, 46, 2201-2205.	5.0	5
102	Formulation and utilization of choline based samples for dissolution dynamic nuclear polarization. Journal of Magnetic Resonance, 2013, 236, 26-30.	2.1	15
103	Magnetic resonance butterfly coils: Design and application for hyperpolarized 13C studies. Measurement: Journal of the International Measurement Confederation, 2013, 46, 3282-3290.	5.0	9
104	Recycling and Imaging of Nuclear Singlet Hyperpolarization. Journal of the American Chemical Society, 2013, 135, 5084-5088.	13.7	94
105	Design of a quadrature surface coil for hyperpolarized <sup>13</sup> C MRS cardiac metabolism studies in pigs. Concepts in Magnetic Resonance Part B, 2013, 43, 69-77.	0.7	9
106	3D CMR Mapping of Metabolism by Hyperpolarized 13C-Pyruvate in Ischemia–Reperfusion. JACC: Cardiovascular Imaging, 2013, 6, 743-744.	5.3	15
107	Metabolic Imaging of Patients with Prostate Cancer Using Hyperpolarized [1- <sup>13</sup> C]Pyruvate. Science Translational Medicine, 2013, 5, 198ra108.	12.4	1,061
108	Hyperpolarized singlet lifetimes of pyruvate in human blood and in the mouse. NMR in Biomedicine, 2013, 26, 1696-1704.	2.8	54

#	Article	IF	CITATIONS
109	Enhancing the [ <sup>13</sup> C]bicarbonate signal in cardiac hyperpolarized [1â€ <sup>13</sup> C]pyruvate MRS studies by infusion of glucose, insulin and potassium. NMR in Biomedicine, 2013, 26, 1496-1500.	2.8	21
110	Cluster formation restricts dynamic nuclear polarization of xenon in solid mixtures. Journal of Chemical Physics, 2012, 137, 104508.	3.0	15
111	Reconstruction methods from hyperpolarized <sup>13</sup> C chemical shift imaging spiral 3D data: Comparison between direct summation and gridding method. , 2012, , .		Ο
112	A novel method for coil efficiency estimation: Validation with a 13C birdcage. Concepts in Magnetic Resonance Part B, 2012, 41B, 139-143.	0.7	2
113	Hyperpolarized <sup>13</sup> C metabolic imaging using dissolution dynamic nuclear polarization. Journal of Magnetic Resonance Imaging, 2012, 36, 1314-1328.	3.4	98
114	Imaging Cerebral 2-Ketoisocaproate Metabolism with Hyperpolarized <sup>13</sup> C Magnetic Resonance Spectroscopic Imaging. Journal of Cerebral Blood Flow and Metabolism, 2012, 32, 1508-1514.	4.3	33
115	Transient decrease in tumor oxygenation after intravenous administration of pyruvate. Magnetic Resonance in Medicine, 2012, 67, 801-807.	3.0	24
116	Hyperpolarized singlet NMR on a small animal imaging system. Magnetic Resonance in Medicine, 2012, 68, 1262-1265.	3.0	37
117	Hyperpolarized 13C MRS Cardiac Metabolism Studies in Pigs: Comparison Between Surface and Volume Radiofrequency Coils. Applied Magnetic Resonance, 2012, 42, 413-428.	1.2	18
118	Coil Sensitivity Estimation with Perturbing Sphere Method: Application to 13C Birdcages. Applied Magnetic Resonance, 2012, 42, 511-518.	1.2	10
119	DNP Methods for Cardiac Metabolic Imaging with Hyperpolarized [1-13C]pyruvate Large Dose Injection in Pigs. Applied Magnetic Resonance, 2012, 43, 299-310.	1.2	12
120	Investigating tumor perfusion and metabolism using multiple hyperpolarized 13C compounds: HP001, pyruvate and urea. Magnetic Resonance Imaging, 2012, 30, 305-311.	1.8	69
121	Assessment of realâ€ŧime myocardial uptake and enzymatic conversion of hyperpolarized [1â€ <sup>13</sup> C]pyruvate in pigs using slice selective magnetic resonance spectroscopy. Contrast Media and Molecular Imaging, 2012, 7, 85-94.	0.8	40
122	Effects of pyruvate dose on <i>in vivo</i> metabolism and quantification of hyperpolarized <sup>13</sup> C spectra. NMR in Biomedicine, 2012, 25, 142-151.	2.8	22
123	How the signalâ€toâ€noise ratio influences hyperpolarized <sup>13</sup> C dynamic MRS data fitting and parameter estimation. NMR in Biomedicine, 2012, 25, 925-934.	2.8	18
124	Metabolism of hyperpolarized [1â€< sup>13C]pyruvate in the isolated perfused rat lung – an ischemia study. NMR in Biomedicine, 2012, 25, 1113-1118.	2.8	18
125	Detection of 3D Cardiac metabolism after injection of hyperpolarized [1-13C]pyruvate. Journal of Cardiovascular Magnetic Resonance, 2011, 13, .	3.3	4
126	Comparison between volume and surface coils for pig cardiac metabolism studies with hyperpolarized 13C MRS. Journal of Cardiovascular Magnetic Resonance, 2011, 13, .	3.3	1

#	Article	IF	CITATIONS
127	Imaging of blood flow using hyperpolarized [ <sup>13</sup> C]Urea in preclinical cancer models. Journal of Magnetic Resonance Imaging, 2011, 33, 692-697.	3.4	105
128	Measurements of the persistent singlet state of N <sub>2</sub> O in blood and other solvents—Potential as a magnetic tracer. Magnetic Resonance in Medicine, 2011, 66, 1177-1180.	3.0	34
129	Quantitative dynamic nuclear polarizationâ€NMR on blood plasma for assays of drug metabolism. NMR in Biomedicine, 2011, 24, 96-103.	2.8	37
130	Dynamic nuclear polarization polarizer for sterile use intent. NMR in Biomedicine, 2011, 24, 927-932.	2.8	204
131	Use of the Frank sequence in pulsed EPR. Journal of Magnetic Resonance, 2011, 209, 306-309.	2.1	9
132	Hyperpolarized Molecules in Solution. Methods in Molecular Biology, 2011, 771, 205-226.	0.9	10
133	Applications of Hyperpolarized Agents in Solutions. Methods in Molecular Biology, 2011, 771, 655-689.	0.9	4
134	Study of molecular interactions with 13C DNP-NMR. Journal of Magnetic Resonance, 2010, 203, 52-56.	2.1	59
135	Hyperpolarized MRS surface coil: Design and signalâ€toâ€noise ratio estimation. Medical Physics, 2010, 37, 5361-5369.	3.0	24
136	Trityl biradicals and 13C dynamic nuclear polarization. Physical Chemistry Chemical Physics, 2010, 12, 5804.	2.8	52
137	Dynamic Nuclear Polarization of [1-13C]pyruvic acid at 4.6 tesla. Journal of Magnetic Resonance, 2009, 197, 167-175.	2.1	130
138	Detection of low-populated reaction intermediates with hyperpolarized NMR. Chemical Communications, 2009, , 5168.	4.1	44
139	Dynamic Nuclear Polarization with Trityls at 1.2 K. Applied Magnetic Resonance, 2008, 34, 509-522.	1.2	138
140	Magnetic resonance imaging of pH in vivo using hyperpolarized 13C-labelled bicarbonate. Nature, 2008, 453, 940-943.	27.8	796
141	Jet Impingement Melting With Vaporization: A Numerical Study. , 2008, , .		4
142	Detecting tumor response to treatment using hyperpolarized 13C magnetic resonance imaging and spectroscopy. Nature Medicine, 2007, 13, 1382-1387.	30.7	825
143	Metabolic Imaging by Hyperpolarized 13C Magnetic Resonance Imaging for In vivo Tumor Diagnosis. Cancer Research, 2006, 66, 10855-10860.	0.9	602
144	Generating highly polarized nuclear spins in solution using dynamic nuclear polarization. Nuclear Instruments and Methods in Physics Research, Section A: Accelerators, Spectrometers, Detectors and Associated Equipment, 2004, 526, 173-181.	1.6	141

#	Article	IF	CITATIONS
145	Increase in signal-to-noise ratio of > 10,000 times in liquid-state NMR. Proceedings of the National Academy of Sciences of the United States of America, 2003, 100, 10158-10163.	7.1	2,484
146	Molecular imaging with endogenous substances. Proceedings of the National Academy of Sciences of the United States of America, 2003, 100, 10435-10439.	7.1	390
147	Increase of signal-to-noise of more than 10,000 times in liquid state NMR. Discovery Medicine, 2003, 3, 37-9.	0.5	11
148	Overhauser enhanced magnetic resonance imaging for tumor oximetry: Coregistration of tumor anatomy and tissue oxygen concentration. Proceedings of the National Academy of Sciences of the United States of America, 2002, 99, 2216-2221.	7.1	284
149	Low field Overhauser images of the formation process of a hydrogel. Applied Physics Letters, 2002, 80, 160-162.	3.3	5
150	13C-Angiography. Academic Radiology, 2002, 9, S507-S510.	2.5	36
151	Three-dimensional whole body imaging of spin probes in mice by time-domain radiofrequency electron paramagnetic resonance. Magnetic Resonance in Medicine, 2000, 43, 375-382.	3.0	58
152	High-Frequency Dynamic Nuclear Polarization in the Nuclear Rotating Frame. Journal of Magnetic Resonance, 2000, 144, 134-141.	2.1	37
153	Dynamic in vivo oxymetry using overhauser enhanced MR imaging. Journal of Magnetic Resonance Imaging, 2000, 12, 929-938.	3.4	105
154	Manganese Dipyridoxyl Diphosphate: MRI Contrast Agent with Antioxidative and Cardioprotective Properties?. Biochemical and Biophysical Research Communications, 1999, 254, 768-772.	2.1	64
155	Overhauser-enhanced MR imaging (OMRI). Acta Radiologica, 1998, 39, 10-17.	1.1	58
156	Electron paramagnetic resonance and dynamic nuclear polarization of char suspensions: surface science and oximetry. Physics in Medicine and Biology, 1998, 43, 1907-1920.	3.0	54
157	Overhauser-enhanced MR imaging (omri). Acta Radiologica, 1998, 39, 10-17.	1.1	6
158	In vivo imaging of a stable paramagnetic probe by pulsed-radiofrequency electron paramagnetic resonance spectroscopy. Magnetic Resonance in Medicine, 1997, 38, 409-414.	3.0	84
159	Line widths in nitroxides. Research on Chemical Intermediates, 1996, 22, 417-425.	2.7	3
160	<scp>RF</scp> coil design for accurate parallel imaging on <scp> <sup>13</sup> C MRSI </scp> using <scp> <sup>23</sup> Na </scp> sensitivity profiles. Magnetic Resonance in Medicine, 0, , .	3.0	5